Bioinspiration & Biomimetics

CrossMark

RECEIVED
25 October 2016

REVISED
14 January 2017

ACCEPTED FOR PUBLICATION
13 February 2017

PUBLISHED
17 March 2017

PAPER

Lightweight 3D cellular composites inspired by balsa

Sardar Malek[1], **Jordan R Raney**[2], **Jennifer A Lewis**[3] **and Lorna J Gibson**[1]

[1] Department of Materials Science and Engineering, Massachusetts Institute of Technology Cambridge, MA 02139, United States of America

[2] Department of Mechanical Engineering and Applied Mechanics, University of Pennsylvania, Philadelphia, PA 19104, United States of America

[3] John A Paulson School of Engineering and Applies Sciences, Wyss Institute for Biologically Inspired Engineering Harvard University Cambridge, MA 02138, United States of America

E-mail: ljgibson@mit.edu

Keywords: composites, 3D printing, multi-scale modeling, finite element method, bioinspired materials, balsa

Abstract

Additive manufacturing technologies offer new ways to fabricate cellular materials with composite cell walls, mimicking the structure and mechanical properties of woods. However, materials limitations and a lack of design tools have confined the usefulness of 3D printed cellular materials. We develop new carbon fiber reinforced, epoxy inks for 3D printing which result in printed materials with longitudinal Young's modulus up to 57 GPa (exceeding the longitudinal modulus of wood cell wall material). To guide the design of hierarchical cellular materials, we developed a parameterized, multi-scale, finite element model. Computational homogenization based on finite element simulations at multiple length scales is employed to obtain the elastic properties of the material at multiple length scales. Parameters affecting the elastic response of cellular composites, such as the volume fraction, orientation distribution, and aspect ratio of fibers within the cell walls as well as the cell geometry and relative density are included in the model. To validate the model, experiments are conducted on both solid carbon fiber/epoxy composites and cellular structures made from them, showing excellent agreement with computational multi-scale model predictions, both at the cell-wall and at the cellular-structure levels. Using the model, cellular structures are designed and experimentally shown to achieve a specific stiffness nearly as high as that observed in balsa wood. The good agreement between the multi-scale model predictions and experimental data provides confidence in the practical utility of this model as a tool for designing novel 3D cellular composites with unprecedented specific elastic properties.

1. Introduction

With inspiration from biological materials, such as wood, coupled with recent advances in additive manufacturing techniques, the fabrication of lightweight cellular structures with improved mechanical properties resulting from fiber-reinforced composite cell walls is becoming possible (Compton and Lewis 2014, Matsuzaki *et al* 2016).

Woods are honeycomb-like cellular materials with fiber-reinforced cell walls. Among woods, balsa (*Ochroma pyramidale*) has remarkable mechanical properties for its weight: for instance, its specific Young's modulus and bending strength are comparable to those of engineering fiber composites (Borrega and Gibson 2015, Malek and Gibson 2017). Its high specific shear modulus and strength are widely exploited in the cores of structural sandwich panels (for instance, in wind turbine rotor blades). Balsa wood is composed of three types of cells: fibers, rays and vessels. Fiber cells, which provide most of the structural support to the tree, are roughly hexagonal honeycombs while ray cells, which store sugars, are more or less rectangular honeycombs. The thin-walled, cylindrical vessel cells conduct fluids through the tree, but do not provide structural support. In both fiber and ray cells, the cell walls are multi-layered: each layer is a composite material consisting of highly crystalline cellulose microfibrils embedded within a matrix of lignin and hemicellulose (Dinwoodie 1981, Bodig and Jayne 1982, Borrega *et al* 2015). Each layer has a different volume fraction and orientation of cellulose microfibrils and a different thickness.

Due to the complex microstructure of woods, researchers have employed mostly computational (finite element) models to understand the mechanical properties of different wood species. Several multi-

© 2017 IOP Publishing Ltd

scale models based on homogenization techniques have been developed to explain the wide range of stiffness and strength values of softwoods (e.g. Hofstetter *et al* (2005), Hofstetter and Gamstedt (2009), Qing and Mishnaevsky (2009, 2010) and Gereke *et al* (2011)) as well as balsa (Shishkina *et al* 2014, Malek and Gibson 2017). The high degree of crystallinity and the low angle, spiral alignment of the cellulose microfibrils along the longitudinal axis of the tree in the thickest cell wall layer (the S2 layer) are the main factors contributing to balsa's remarkably high specific Young's moduli.

Additive manufacturing technologies offer new approaches for fabricating bio-inspired composites that mimic the structure and mechanical properties of natural materials like balsa wood (Compton and Lewis 2014, Studart 2016). Notably, they enable fabrication of composite parts with complex shapes without the use of expensive molds (Raney and Lewis 2015, Matsuzaki *et al* 2016). However, most commercially available materials for 3D printing do not possess the mechanical properties necessary to compete with traditional structural composites. Direct ink writing, a technique in which viscoelastic inks are extruded through fine deposition nozzles to create 3D structures in a layer-by-layer manner, is a 3D printing approach for which a large materials palette has been developed, enabling the precise patterning of polymeric, ceramic, and metallic systems (Smay *et al* 2002, Gratson *et al* 2004, Ahn *et al* 2009). Recently, an epoxy-based ink for direct writing was developed by Compton and Lewis (2014), enabling the fabrication of hierarchical composite structures with orthotropic cell walls inspired by balsa wood. They demonstrated that fibers with modest aspect ratios (i.e. $L/D = 22$) readily aligned under the shear and extensional flow field within the micro-nozzle during printing, producing composite structures with aligned carbon fibers and silicon carbide whiskers. However, a low volume fraction of carbon fibers in the ink limited the maximum achievable stiffness in the printed structures. Here, we expand upon this approach in two important ways: (1) the volume fraction of carbon fibers used is nearly a factor of six higher, leading to the 3D printing of cellular materials of exceptional specific stiffness (comparable to balsa wood); and (2) only carbon fiber fillers are used to achieve a simplified microstructure (i.e. without silicon carbide whiskers) that is far more amenable to both analytical and numerical modeling.

Although 3D printing of composites offers flexibility in designing lightweight cellular structures with high specific mechanical properties, optimal design of such materials for a specific application (or load condition) requires developing versatile multi-scale models (Raney and Lewis 2015). As we show below, the analytical equations developed for the effective elastic properties of honeycombs with isotropic cell walls (Malek and Gibson 2015) give only rough estimates of the effective elastic properties of materials with composite walls. More advanced models (e.g. numerical, multi-scale models) that can capture the orthotropic nature of the cell walls are required for designing the next generation of composites made with aligned fiber composites in complex 3D architectures, like those reported by Compton and Lewis (2014).

To design bio-inspired hierarchical cellular composites and to understand the effect of various design parameters on their effective elastic properties, we have developed a computational multi-scale model. Using this model, we show how varying different parameters at different levels of microstructural hierarchy affects the effective elastic properties of cellular composites. We also test cellular composites virtually and design cellular structures that exceed the specific elastic properties of balsa wood (the lightest wood) as well as other synthetic cellular materials currently available to engineers.

In section 2, the basis of the 3D multi-scale computational model for designing high-performance cellular composites is described. The unit cells and different design parameters that are included in the model are explained in detail. In section 3, we compare the results of the model with data from experiments conducted on cellular composites with different cell geometries and a wide range of densities. Comparisons are made at both the cell-wall and cellular-structure levels. To investigate the validity range of the analytical models developed for hexagonal and square honeycombs with isotropic cell walls, predictions of the equations previously developed by Malek and Gibson (2015) for honeycombs with thick cell walls are also compared with the data. Only the numerical results give a good description of the elastic behavior of cellular composites over the wide range of densities considered. Finally, the use of the multi-scale computational tool to guide the design of novel materials with high specific elastic properties is discussed in section 4.

2. Methodology

2.1. Basis

A multi-scale approach has recently been developed to study the mechanics of balsa wood (figure 1). At each length scale, a representative unit cell of the material is identified and the effective stiffness matrix is determined using finite element analysis with appropriate periodic boundary conditions. The model represents the main features of the microstructure at each length scale, including the orthotropic properties of cellulose microfibrils, the microfibrillar angle, the thickness of cell wall layers, as well as the geometry and arrangement of the fiber and ray cells (the vessel cells are neglected in this model).

We adapt the multi-scale numerical approach described in Malek and Gibson (2017) to model and design cellular materials with composite cell walls, inspired by balsa. Using a 3D printing approach similar to that developed by Compton and Lewis (2014), cellular composites can be fabricated with different

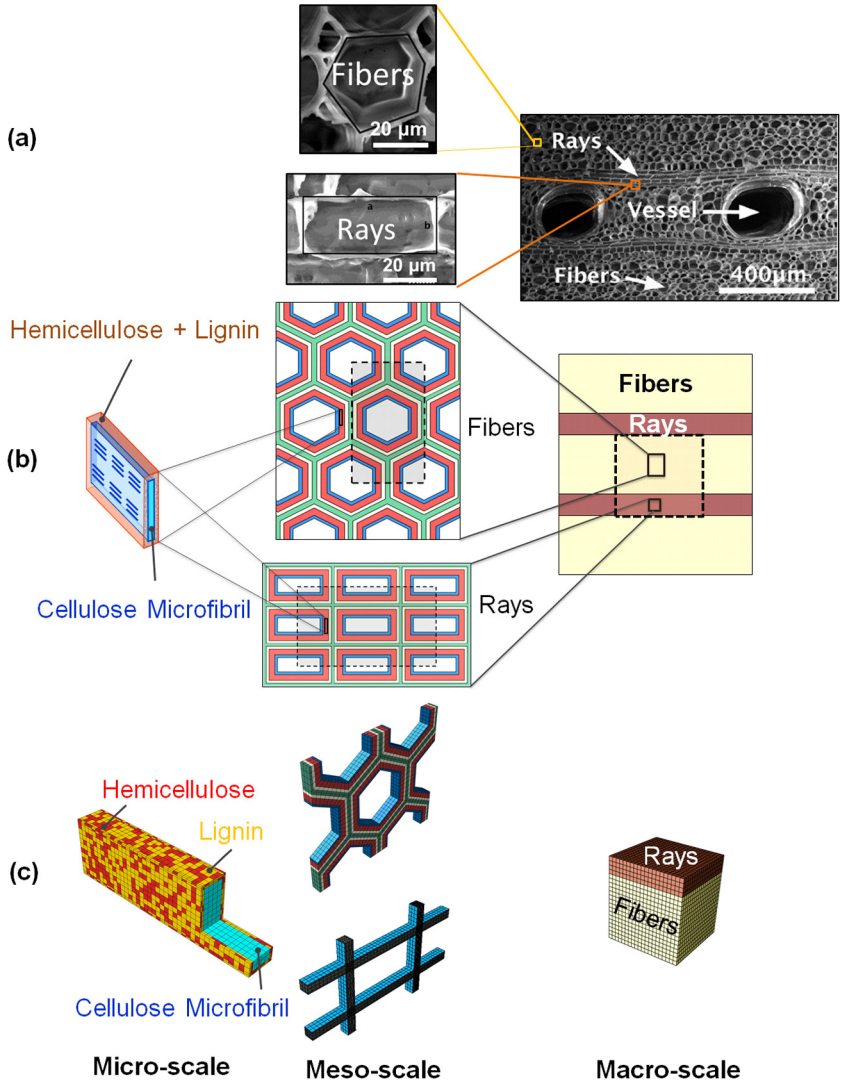

Figure 1. Multi-scale modeling of balsa. (a) SEM micrograph of the structure of balsa. (b) Schematic representation of the hierarchical structure of balsa. (c) Discretized material unit cells at different length scales (Malek and Gibson 2017). The different colors at the meso-scale represent different cell wall layers. SEM images and the schematics are reproduced from Borrega et al (2015) © Springer-Verlag Berlin Heidelberg 2015, with permission of Springer, and Malek and Gibson, Copyright (2017), with permission from Elsevier.

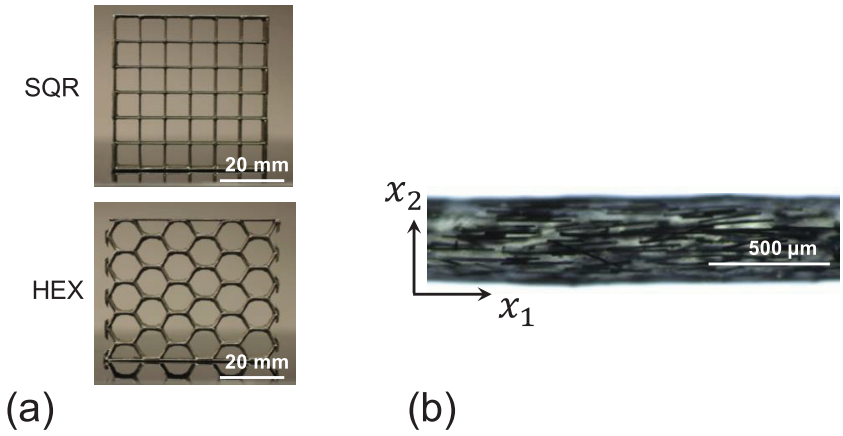

Figure 2. Cellular composites fabricated using 3D printing. (a) Bio-inspired honeycomb structures. (b) Optical image of the cell wall material showing the alignment of high aspect ratio carbon fibers.

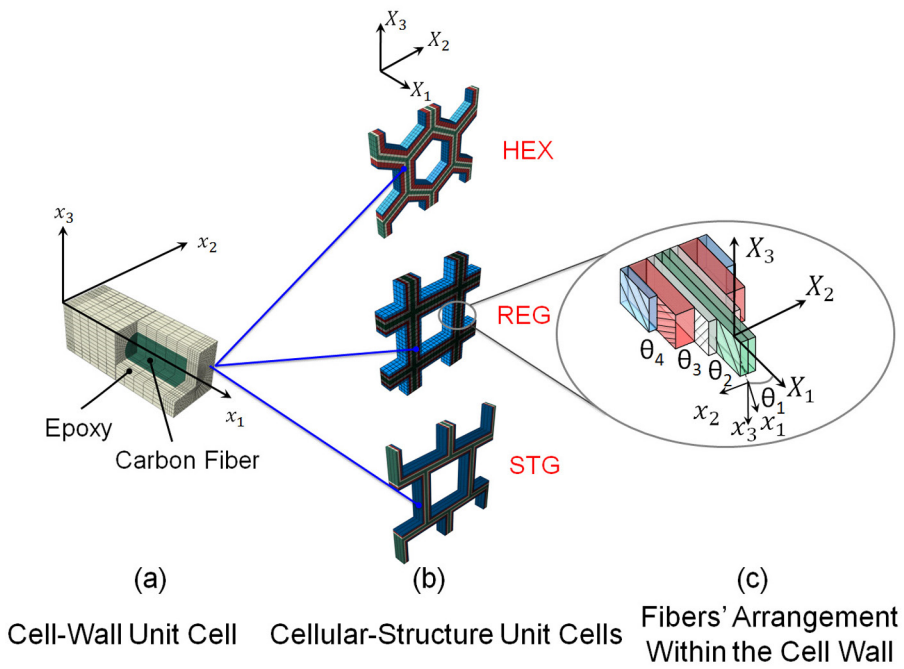

Figure 3. Schematic representation of the multi-scale approach for modelling cellular composites inspired by balsa. The different colors at the cellular-structure level represent eight layers (symmetric or anti-symmetric about the cell wall middle surface) with different orientations of fibers.

levels of hierarchy, similar to balsa (figure 2). Here, we focus on only two levels of hierarchy (i.e. cell-wall and cellular-structure) to demonstrate the accuracy of the model in predicting the effective elastic properties of cellular composites. Considering these two levels of hierarchy enables us to investigate systematically the effect of different design parameters on the overall elastic properties of cellular materials with composite cell walls.

2.2. Modeling approach

Assuming that the material has a periodic structure at each length scale, a unit cell representing the structure of the material at that length scale can be identified. Figure 3 shows the unit cells that are identified and discretized to model the effective elastic properties of cellular composites.

At the cell-wall level, the material consists of aligned short fibers of carbon embedded in an epoxy matrix. Note that axes x_1, x_2 and x_3 in figure 3(a) are local axes, with x_1 oriented along the fiber length, and that X_1, X_2 and X_3 in figures 3(b) and (c), are global axes, with X_1 oriented along the cell prism axis. Assuming square packing for carbon fibers within the cell wall, a unit cell representing the microstructure of the carbon/epoxy composite can be identified (see of figure 3(a)). As we show in section 3.2, the effective elastic properties of this aligned short fiber composite at fiber volume fraction of 13.1% are close to those of balsa's cell wall material.

At the cellular-structure level, the composite can be printed with different cell geometries. Here, we consider periodic hexagonal and rectangular cells, resembling balsa's fiber and ray cells, respectively (see figure 1). To better examine the effect of different parameters, we focus on the elastic properties of three different cell types in printing the cellular composites: regular hexagonal (HEX), and regular (REG) and staggered (STG) square cells (figure 3(b)).

Changing printing parameters may lead to a non-uniform orientation of fibers within the cell wall, which can affect the overall elastic properties of the cellular composite. To include the orientation distribution of fibers in the model, similar to balsa, the cell wall material is divided into eight symmetric (or anti-symmetric) layers; each layer is represented by a different color in figure 3(c). Layers with the same color have the same fiber orientation and layer thickness. The fibers within each layer are assumed to be aligned and their orientation with respect to the longitudinal axis of the cells is denoted by angle θ_i; the subscript i corresponds to the layer i. The elastic properties of each layer are computed employing the unit cell shown in figure 3(a). The material behavior of each layer at the cellular-structure level is defined as generally orthotropic and elastic with a distinct material orientation to represent the orientation of the fibers.

At each scale, finite element simulations using 8-noded linear brick elements, C3D8, are performed on the discretized unit cell in ABAQUS® software (ABAQUS Inc. 2010) to characterize its stiffness matrix and obtain its engineering constants. The effective stiffness matrix of each unit cell is determined by applying six elementary loadings (three uniaxial extensions and three simple shear loadings) corresponding to pre-specified forms of the average strain tensor (see Malekmohammadi (2014) for the details). The orthotropic elastic properties (nine engineering constants) are then determined from the components of the compliance matrix obtained from averaging the local stress field over the unit cell volume.

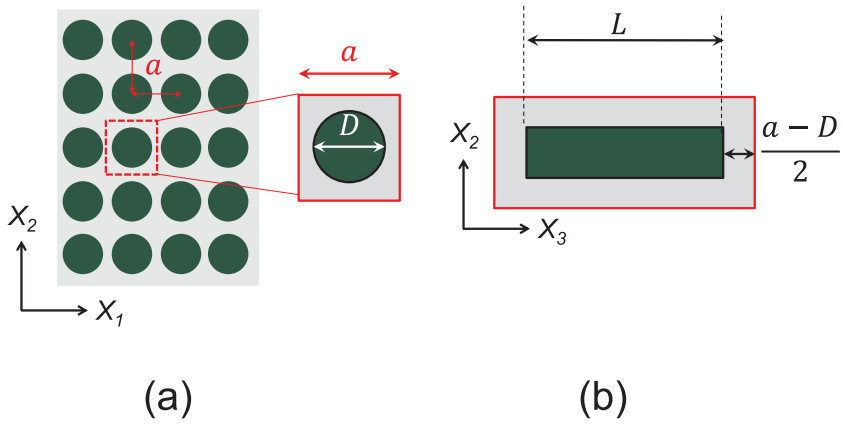

Figure 4. Cell-wall unit cell and its parametrized dimensions. Unit cell cross-sections are shown in (a) X_1-X_2, and (b) X_2-X_3 planes.

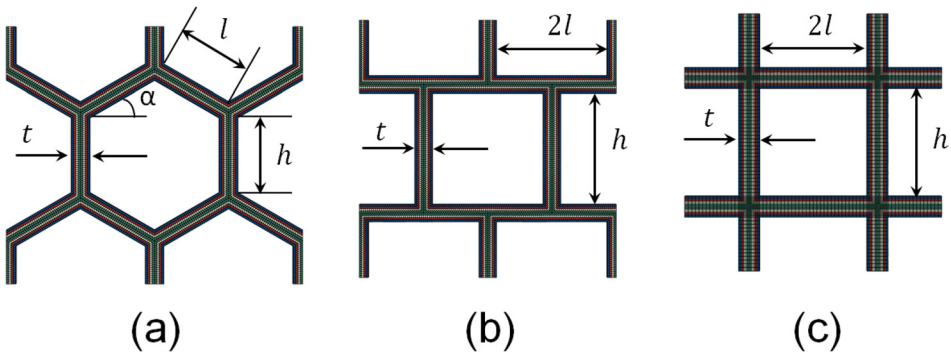

Figure 5. Cellular-structure unit cells and parametrized dimensions characterizing the (a) hexagonal (HEX), (b) staggered (STG), and (c) regular (REG) square cell types. The different colors represent the layers with different fiber orientation angle, θ_i (see figure 3(c)).

2.3. Design parameters

One of the main purposes of developing the current multi-scale model is to analyze quantitatively the effect of different parameters on the effective elastic properties of a cellular structure with a composite cell wall.

The *cell-wall design parameters* are the volume fraction, V_f, and aspect ratio (L/D) of the carbon fibers; these two parameters can be varied while preparing the composite ink for printing cellular composites. A small change in these parameters can affect the cell wall effective elastic properties significantly. The fiber diameter and length, D and L, and the minimum fiber spacing, a, are shown schematically in figure 4. Assuming square fiber packing, they are related to fiber volume fraction, V_f, as follows:

$$V_f = \frac{\pi D^2 L}{4a^2(L + a - D)} \tag{1}$$

The *cellular-structure design parameters* that can be varied while printing the cellular structures are cell wall length, l, height, h, thickness, t (figure 5). At the cellular level, composites may be printed as honeycombs with different cell geometries with varying cell wall angle, α; here we take $\alpha = 30°$ for the hexagonal cells and 0° for the rectangular cells. The fiber orientation angle within the cell wall may also be varied using different printing techniques; to include the orientation distribution of fibers in the model, four different orientation angles denoted by $\theta_i (i = 1, 2, 3, 4)$ are considered (see figure 3).

3. Validations

3.1. Experiments

Both solid and cellular composites are fabricated following a similar approach to that of Compton and Lewis (2014). Inks are developed starting with an epoxy resin (Momentive Epon 826) as the base. Nanoclay (Nanocor I34TCN) is mixed into the resin as a rheological modifier, producing a shear-thinning rheology (convenient for extruding the material through a nozzle) and a viscoelastic yield stress (see figure 6 for rheological measurements, as characterized with a commercial rheometer, TA Instruments AR2000EX), which ensures that extruded material maintains its form until a final curing step. Dimethyl methylphosphonate is added to assist with achieving high solids loading. Short carbon fibers (Dialead K223HM, 220 μm length, 10 μm diameter) are mixed with the above (FlackTek SpeedMixer DAC 600.2 VAC) under vacuum conditions. After mixing, an imidazole-based curing agent (BASF Basionics VS03) is added, with an additional mixing step. Different inks

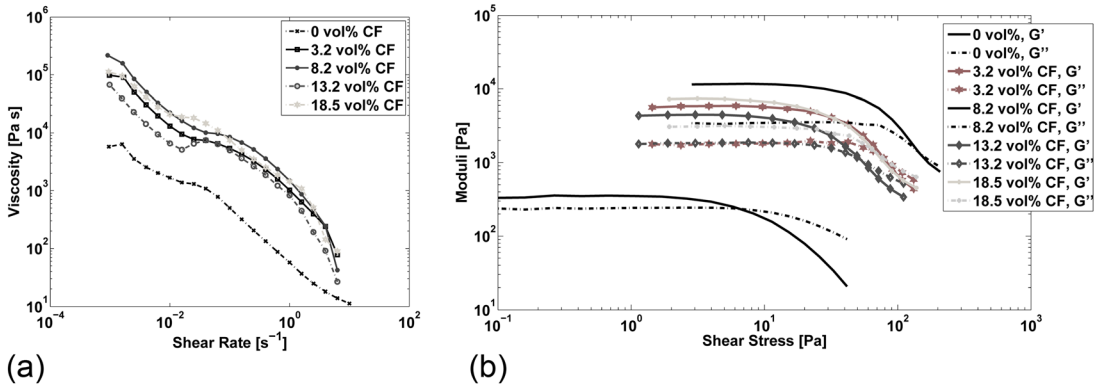

Figure 6. Rheological behavior of epoxy-based inks of varying composition of carbon fibers (CF). (a) Apparent viscosity as a function of shear rate; (b) shear storage and loss moduli as a function of shear stress.

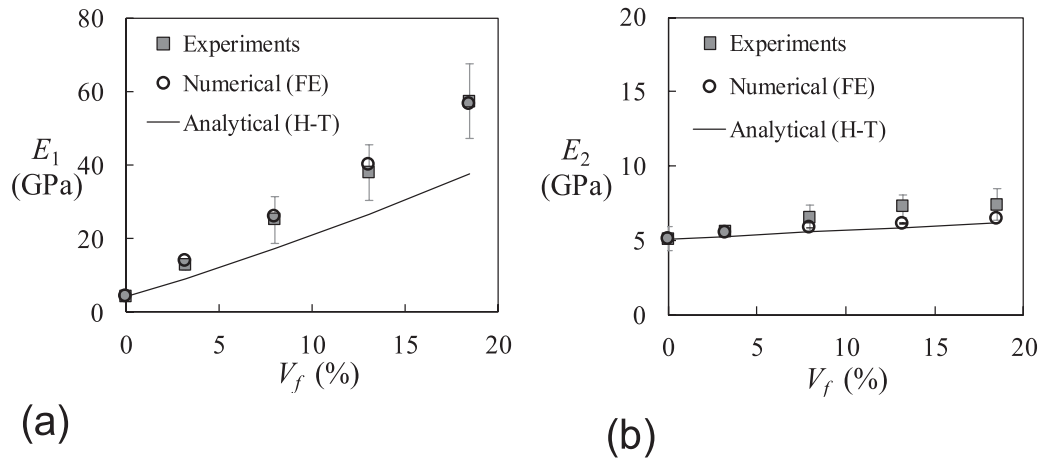

Figure 7. Effective elastic moduli of the composite cell wall material with aligned carbon fibers in epoxy matrix along the (a) fiber direction and (b) perpendicular to the fiber direction (see figure 2(a)). Comparisons between the numerical model shown by circles, analytical model (Halpin–Tsai equations) shown by lines, and experimental data shown by squares. Predictions are given for tensile bars printed with three different volume fractions of carbon fibers.

are fabricated in this way, with carbon fiber volume fractions ranging from 0% to 18.5%. The inks are extruded through tapered nozzles of 610 μm diameter and patterned using a custom 3D motion control system (Aerotech) to produce the desired structures. These structures are subsequently cured in a two-step process: 100 °C for 15 h followed by 220 °C for 2 h.

First, solid tensile specimens are 3D printed with inks of varying carbon fiber volume fraction. To investigate the effects of fiber orientation, tensile bars are printed using two different printing paths: one oriented longitudinally along the tensile direction and the other oriented transverse to the tensile direction. Tension is applied using a commercial quasi-static test system (Instron model 4201) at a strain rate of approximately 10^{-5} s^{-1}. Sample strain is monitored during loading using an LVDT strain sensor (Instron).

Using an ink with 13.1 vol% carbon fibers, cellular structures are 3D printed with a nozzle of diameter 610 μm. As shown in figure 2, the fibers are aligned in the print direction due to the shear effects in the nozzle; i.e. $\theta_i = 90°(i = 1, 2, 3, 4)$ in figure 3(c). The samples possess 5–6 cells along each dimension; a previous study examining boundary effects of such samples indicated that their Young's modulus is 90% of that for an infinite number of cells (Onck *et al* 2001). To measure the overall elastic properties of cellular composites, we used a commercial system (Instron 5566) to subject the cellular structures to in-plane compression tests at strain rates of approximately 2×10^{-4} s^{-1}, loading in the X_3 direction (figure 3), for samples printed with a range of cell sizes and relative densities. Prior to testing, surfaces of the specimens are ground flat to ensure uniform contact with the compression platens. Small dots are painted on the specimen to allow contactless monitoring via a camera of both global and local strain during loading. The in-plane modulus of specimens in the X_3 direction is obtained from the slope of the load-deflection curve. The density is calculated from the measured mass and volume of each specimen.

Table 1. Comparison between specific Young's moduli of the new composite ink (epoxy/CF), its constituents, and balsa's cell wall material.

Material	E (GPa)	ρ (kg m^{-3})	E/ρ MPa (kg/m^3)$^{-1}$
Epoxy	4.14	1300	3.2
Carbon fiber (CF)[a]	900	2200	409.1
Composite (epoxy/CF) cell wall	38.1	1420	26.9
Balsa cell wall (at moisture content of 6%)[b]	41	1560	26.3

[a] Compton and Lewis (2014).
[b] Borrega and Gibson (2015).

3.2. Results

Figure 7 shows the comparison for the Young's moduli of the solid cell wall material printed using epoxy inks filled with different volume fractions of carbon fibers, for loading along and across the fibers. At fiber volume fraction of 13.1%, the effective Young's moduli of the carbon/epoxy composite are 38.1 and 7.3 GPa in longitudinal and transverse directions, respectively. These values are comparable to measured values of the longitudinal and transverse moduli of wood (*Pinus radiata*) cell wall (35 GPa and 10 GPa (Cave 1968)) and model values for balsa wood (45 and 7 GPa (Malek and Gibson (2017)). Table 1 compares the specific longitudinal Young's modulus of balsa's cell wall material, measured by Borrega and Gibson (2015) at moisture content of 6%, with epoxy, carbon fiber and the solid ink that we selected for printing cellular composites. Note that carbon fiber has a very high specific longitudinal Young's modulus compared to epoxy and the natural cell wall material in balsa. This would enable us to fabricate composites with carbon fibers that exceed the specific Young's modulus of balsa's cell wall material (a natural composite of cellulose microfibrils with lower Young's modulus embedded in a matrix of lignin and hemicellulose). Despite a significantly higher stiffness at higher volume fractions (57 GPa at 18.5%), we chose the 13.1% formulation for printing cellular structures in this study, both due to its similarities to wood cell wall and because of its superior printability (fewer instances of nozzle clogging than observed at higher filler volume fractions). The finite element results give a very good description of the measured Young's moduli of the cell wall material in both longitudinal (figure 7(a)) and transverse (figure 7(b)) directions. Analytical estimates using Halpin–Tsai equations (Halpin and Kardos 1976) are also given for comparison. Figure 7 shows that by increasing the volume fraction of carbon fibers, the discrepancy between the analytical model and both the numerical model and experimental data increases. In general, the accuracy of Halpin–Tsai equations in predicting the elastic properties of aligned short fiber composites decreases as the volume fraction of fiber or the mismatch between fiber and matrix elastic moduli increases. The 3D numerical model, capturing the local stress and strain fields and providing more accurate estimates of the effective elastic properties of solid composites, is used in this paper.

Data for the in-plane Young's modulus, E_3, of the cellular structures printed with carbon fibers approximately aligned with the print direction ($\theta_i = 90°$) are plotted against their density in figure 8, along with predictions using the computational model described in this paper, as well as those of analytical equations by Malek and Gibson (2015). The analytical equation used for hexagonal cells (HEX) and staggered square cells (STG) is (Malek and Gibson 2015):

$$E_3^* = (E_1)_s\left(\frac{t}{l_b}\right)^3 \frac{(h/l + \sin\alpha)}{\cos^3\alpha} \times \left[\frac{1}{1 + \left(2.4 + 1.5(\nu_{12})_s + \tan^2\alpha + \frac{2(h_b/l_b)}{\cos^2\alpha}\right)\left(\frac{t}{l_b}\right)^2}\right] \quad (2)$$

where t is the cell wall thickness, $(E_1)_s$ and $(\nu_{12})_s$ are Young's modulus and Poisson's ratio of the solid composite material for loading in the fiber direction. The effective lengths of the inclined and vertical cell walls (l_b and h_b, respectively) which bend under in-plane loading are defined as:

$$l_b = l - t/(2\cos\alpha), \quad h_b = h - t(1 - \sin\alpha)/\cos\alpha \quad (3)$$

In equations (2) and (3), α, the angle between the horizontal and the inclined cell wall, is equal to 30° and 0° for HEX and STG geometries, respectively. Note that the above equations are only valid for honeycomb structures with $t < l$ ($\rho^* = 1000$ kg m^{-3}). If $t \geqslant l$, some areas that were considered in deriving the above equations overlap each other so that the structure is no longer a honeycomb and the equations obtained in Malek and Gibson (2015) are not applicable.

The in-plane Young's modulus, E_3 of regular square cells (REG), is estimated by:

$$E_3 = (E_1)_s\left(\frac{t}{l}\right) \quad (4)$$

The regular square cells (REG) deform by axial compression along the aligned cell walls, leading to a slope of the plot of close to 1, while the hexagonal cells (HEX) and staggered square cells (STG) deform mainly by bending of the cell walls, leading to a slope of close to 3. The REG cells are much stiffer than the STG or HEX cells in the X_3 direction, especially at lower densities. Note that due to the symmetry of regular square and hexagonal cells, E_2 and E_3 are equal. The elastic moduli of STG cells in the X_2 direction are equal to those of REG cells.

The lower intercept for the numerical and experimental results relative to those of analytical ones in figure 8 can be explained by the orthotropic nature of cell wall material. The stiffness matrix components of an orthotropic material depend not only on the elastic properties of the material in one direction but also

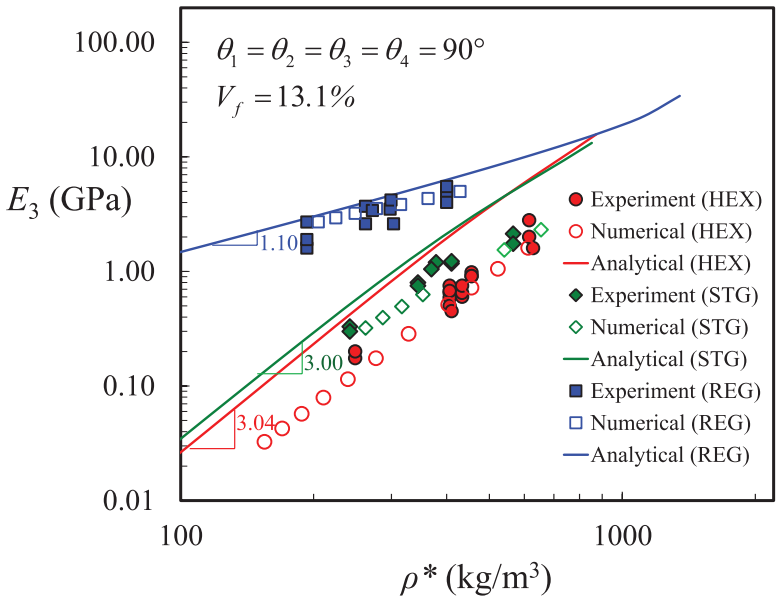

Figure 8. Elastic moduli of printed cellular composites versus density. Comparisons between the numerical model predictions shown by open symbols, analytical model (Malek and Gibson 2015) by lines, and experimental data shown by filled symbols. Note that the analytical model assumes isotropic cell walls with $E_1 = E_2 = E_3 = 38.1$ GPa and $\nu = 0.3$.

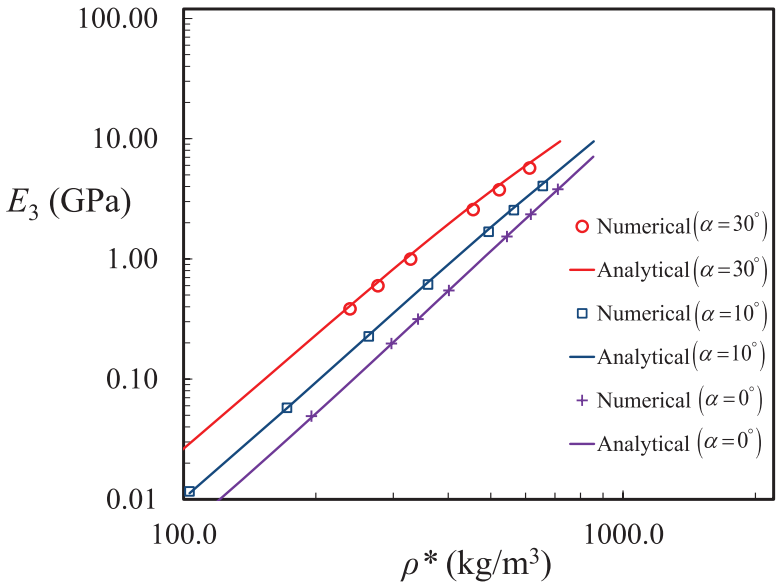

Figure 9. Elastic moduli of periodic honeycombs with hypothetical isotropic cell walls (cell wall properties: $E_1 = E_2 = E_3 = 38.1$ GPa and $\nu = 0.3$) versus density. Comparisons between the numerical model predictions shown by open symbols and analytical model (Malek and Gibson 2015) by lines. Data are plotted for hexagonal honeycombs with $h = l$ at different inclination angles, i.e. $\alpha = 0°, 10°, 30°$.

on those in other directions and the coupling between them. The analytical equations were derived assuming that the cell wall material is isotropic, which for our printed cellular structures is not valid. To better illustrate this effect, numerical simulations are conducted with an isotropic cell wall material with $(E_1)_s = 38.1$ GPa and $(\nu_{12})_s = 0.3$. In figure 9, results are compared with analytical predictions of equation (2) at three different cell geometry inclination angles and a wide range of densities. The very good agreement between analytical predictions and numerical results indicates the high accuracy of analytical equations for honeycombs with isotropic cell walls. Furthermore, the significant difference between numerical results in figures 8 and 9 for hexagonal honeycombs reveals that such analytical equations can only be employed for estimating the effective properties of cellular structures with isotropic cell walls.

Measuring all elastic moduli of cellular composites is both costly and time-consuming. To demonstrate the application of the computational model for designing cellular composites, the effective Young's and shear moduli of cellular composites with REG cells and different fiber orientation angles are estimated

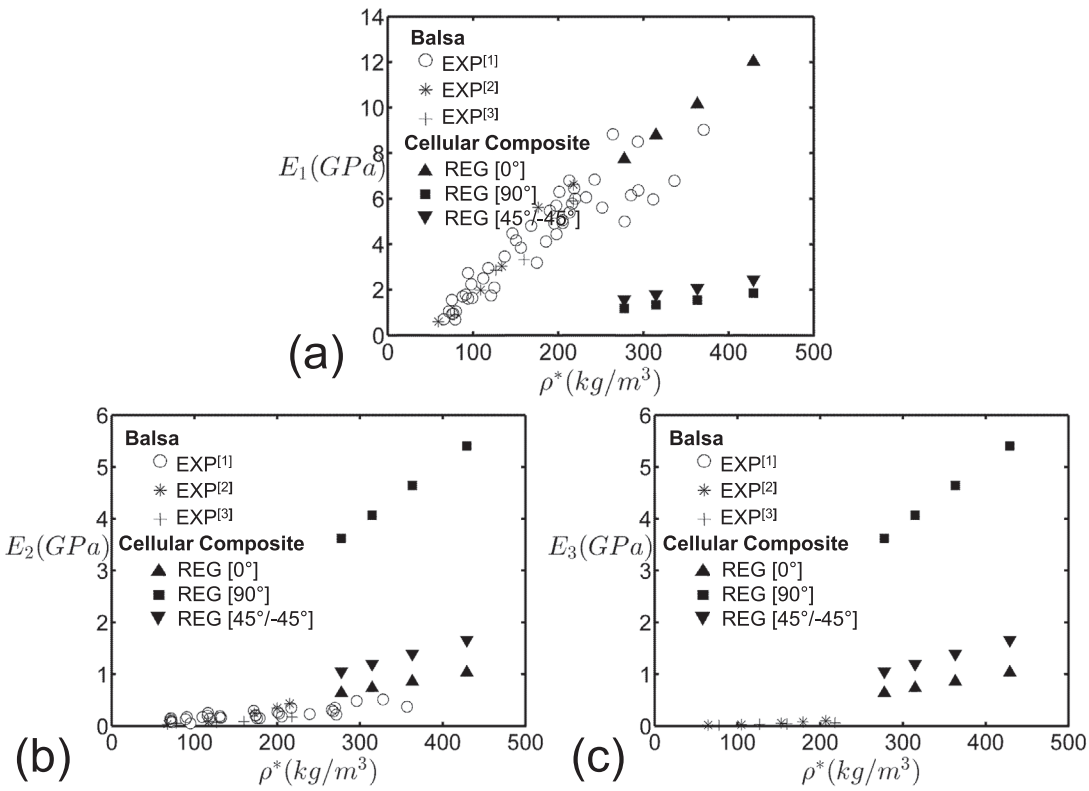

Figure 10. Effective Young's moduli of bio-inspired REG cellular composites of epoxy/carbon with $V_f = 13.1\%$ and balsa in the (a) X_1 (axial), (b) X_2 (radial), and (c) X_3 tangential directions as a function of density. The orientation of the fibers within the cell wall material (with respect to the longitudinal axis of the cells) is given in the brackets. The experimental data are taken from measurements by: (1) Borrega and Gibson (2015) at MC = 5–7%; (2) Da Silva and Kyriakides (2007) at MC = 9–12%; (3) Easterling *et al* (1982) at MC = 12%. Adapted from Malek and Gibson 2017, Copyright (2017), with permission from Elsevier.

(figures 10 and 11). The REG cell geometry was chosen as it produces axial deformation in the cell walls for loading in the X_1, X_2 and X_3 directions. The carbon fiber content in the cell wall material of the cellular structures is assumed to be 13.1%, similar to those in figure 7. In these figures, the reported Young's and shear moduli of balsa wood with different densities are also given for comparison; the balsa data are taken from measurements by Easterling *et al* (1982), Da Silva and Kyriakides (2007) and Borrega and Gibson (2015).

Figure 10(a) shows that by orienting the fibers in the X_1 direction ($\theta = 0°$), the cellular composites match the specific out-of-plane Young's and shear moduli of balsa (i.e. ~27 MPa (kg/m^3)$^{-1}$ for Young's and 1.1 MPa (kg/m^3)$^{-1}$ for shear moduli). Furthermore, the specific in-plane Young's moduli of the REG cellular structures we printed, with a volume fraction of fibers of 13.1% and $\theta = 90°$, (12–13 MPa (kg/m^3)$^{-1}$) exceed those of balsa (~1–2 MPa (kg/m^3)$^{-1}$ by about an order of magnitude. In terms of shear moduli, cellular structures with carbon/epoxy cell walls with $\theta = \pm 45°$ have effective out-of-plane shear moduli more than three times those of balsa at comparable density (figures 11(a) and (b)). Hence, the specific out-of-shear moduli of these cellular composites can be increased significantly, from 1.1 MPa (kg/m^3)$^{-1}$ to 3.6 MPa (kg/m^3)$^{-1}$, by aligning the fibers close to $\theta = \pm 45°$.

4. Discussion

The computational model predictions give a good description of the experimental data for the in-plane Young's moduli of the 3D printed cellular composites with different cell geometries and densities. This validates the current multi-scale modeling approach in designing periodic cellular composites with high specific stiffness.

For E_3, multi-scale model predictions (validated by experiments in figure 8) show that using the same ink (carbon/epoxy inks with $V_f = 13.1\%$), only cellular composites printed with REG cells have higher specific in-plane Young's moduli than those of balsa. By orienting the carbon fibers along the in-plane load direction, the specific in-plane Young's modulus of cellular composites can exceed those of balsa by more than six times (figure 10(b)). The cellular composites with fibers oriented at $\theta = \pm 45°$ also have higher specific out-of-plane shear moduli than balsa (figures 11(a) and (b)), making them more effective for the cores of lightweight structural sandwich panels, one of the main applications of balsa.

The development of techniques enabling control of the orientation of fibers during printing can lead to novel materials with much higher specific elastic properties than conventional cellular materials. The

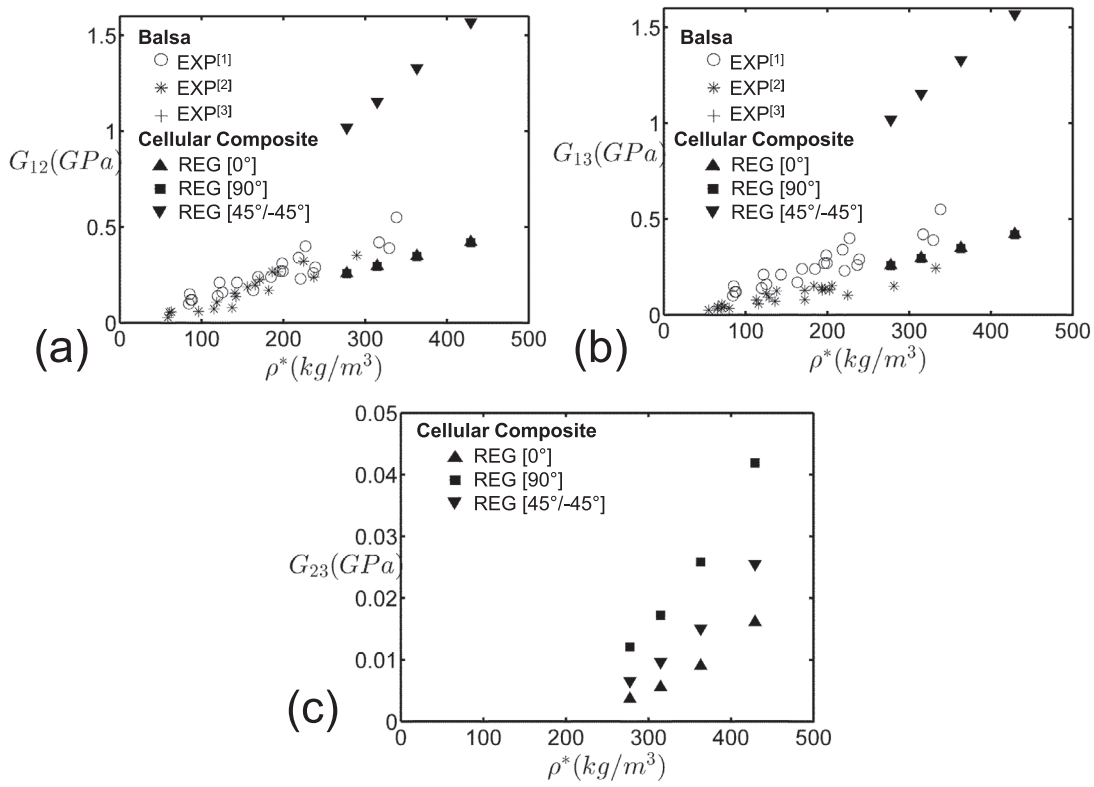

Figure 11. Effective shear moduli of bio-inspired REG cellular composites of carbon/epoxy with $V_f = 13.1\%$ and balsa in the (a) $X_1 - X_2$, (b) $X_1 - X_3$, and (c) X_2-X_3 planes as a function of density. The orientation of the fibers within the cell wall material (with respect to the longitudinal axis of the cells) is given in the brackets. The experimental data are taken from measurements by: (1) Borrega and Gibson (2015) at MC = 5–7%; (2) Da Silva and Kyriakides (2007) at MC = 9–12%; (3) Easterling *et al* (1982) at MC = 12%. Adapted from Malek and Gibson 2017, Copyright (2017), with permission from Elsevier.

multi-scale computational modeling tool presented here provides guidance in the development of high-performance materials that expand the available range of properties of cellular materials.

5. Conclusion

Cellular composites with periodic architectures are an emerging class of structural materials. Natural cellular materials show remarkable specific stiffness and other desirable properties. While additive manufacturing offers the potential to produce synthetic cellular composites with similar properties, this has been limited by poor commercial materials and lack of effective design tools. We have developed a series of carbon fiber-filled epoxy inks that enable the 3D printing of structures with specific stiffness on the order of balsa. To design hierarchical cellular composites with optimized effective elastic properties, a multi-scale model based on computational homogenization is developed in this work. Cellular composites with different densities and architectures (cell types) are fabricated with 3D printing and tested to validate the model. The results showed that by controlling only the fiber orientations and cell geometries in the printing process, we can enhance the specific elastic moduli of cellular structures made with aligned short fiber composites of carbon and epoxy. Importantly, the model can also be used to design cellular materials with elastic properties significantly higher than those of balsa wood.

Acknowledgments

Financial support from BASF through the North American Center for Research on Advanced Materials (Program Manager Dr Marc Schroeder; Project Managers: Dr Holger Ruckdaeschel and Dr Rene Arbter) is gratefully acknowledged. JAL gratefully acknowledges support from the Vannevar Bush Faculty Fellowship program sponsored by the Basic Research Office of the Assistant Secretary of Defense for Research and Engineering and funded by the Office of Naval Research through grant N00014-16-1-2823 and the Wyss Institute for Biologically Inspired Engineering.

References

Ahn B Y, Duoss E B, Motala M J, Guo X, Park S-I, Xiong Y, Yoon J, Nuzzo R G Rogers J A and Lewis J A 2009 Omnidirectional printing of flexible, stretchable, and spanning silver microelectrodes *Science* **323** 1590–3

Bodig J and Jayne B A 1982 *Mechanics of Wood and Wood Composites* (New York: Van Nostrand Reinhold)

Borrega M, Ahvenainen P, Serimaa R and Gibson L 2015 Composition and structure of balsa (Ochroma pyramidale) wood *Wood Sci. Technol.* **49** 403–20

Borrega M and Gibson L J 2015 Mechanics of balsa (ochroma pyramidale) wood *Mech. Mater.* **84** 75–90
Cave I D 1969 The longitudinal Young's modulus of *Pinus Radiata Wood Sci. Technol.* **3** 40–48
Compton B G and Lewis J A 2014 3D-printing of lightweight cellular composites *Adv. Mater.* **26** 5930–5
Da Silva A and Kyriakides S 2007 Compressive response and failure of balsa wood *Int. J. Solids Struct.* **44** 8685–717
Desch H E and Dinwoodie J M 1981 *Timber: its Structure, Properties and Utilisation* A 6th Edition (London: Macmillan)
Easterling K E, Harrysson R, Gibson L J and Ashby M F 1982 On the mechanics of balsa and other woods *Proc. R. Soc.* A **383** 31–41
Gereke T, Malekmohammadi S, Nadot-Martin C, Dai C, Ellyin F and Vaziri R 2011 A numerical multiscale approach for stiffness predictions of wood composite *Proc. 26th Annual Technical Conf. American Soc. for Composites-The 2nd Joint US-Canada Conf. Composites,* (Montreal, Quebec, Canada)
Gratson G M, Xu M and Lewis J A 2004 Microperiodic structures: direct writing of three-dimensional webs *Nature* **428** 386
Halpin J C and Kardos J L 1976 The Halpin–Tsai equations: a review *Polym. Eng. Sci.* **16** 344–52
Hofstetter K and Gamstedt E K 2009 Hierarchical modelling of microstructural effects on mechanical properties of wood. A review COST Action E35 2004–2008: Wood machining—micromechanics and fracture *Holzforschung* **63** 130–8
Hofstetter K, Hellmich C and Eberhardsteiner J 2005 Development and experimental validation of a continuum micromechanics model for the elasticity of wood *Eur. J. Mech.* A **24** 1030–53
Malek S and Gibson L 2015 Effective elastic properties of periodic hexagonal honeycombs *Mech. Mater.* **91** 226–40
Malek S and Gibson L 2017 Multi-scale modelling of elastic properties of balsa *Int. J. Solids Struct.* https://doi.org/10.1016/j.ijsolstr.2017.01.037
Malekmohammadi S 2014 Efficient Multi-Scale Modelling of Viscoelastic Composites with Different Microstructures *PhD Thesis* (Department of Civil Engineering, The University of British Columbia, Vancouver, Canada)
Matsuzaki R, Ueda M, Namiki M, Jeong T-K, Asahara H, Horiguchi K, Nakamura T, Todoroki A and Hirano Y 2016 Three-dimensional printing of continuous-fiber composites by in-nozzle impregnation *Sci. Rep.* **6** 23058
Onck P R, Andrews E W and Gibson L J 2001 Size effects in ductile cellular solids. Part I: modelling *Int. J. Mech. Sci.* **43** 681–99
Qing H and Mishnaevsky L 2009 3D hierarchical computational model of wood as a cellular material with fibril reinforced, heterogeneous multiple layers *Mech. Mater.* **41** 1034–49
Qing H and Mishnaevsky L 2010 3D multiscale micromechanical model of wood: From annual rings to microfibrils *Int. J. Solids Struct.* **47** 1253–67
Raney J R and Lewis J A 2015 Printing mesoscale architectures *MRS Bull.* **40** 943–50
Shishkina O, Lomov S V, Verpoest I and Gorbatikh L 2014 Structure–property relations for balsa wood as a function of density: modelling approach *Arch. Appl. Mech.* **84** 789–805
Smay J E, Cesarano J and Lewis J A 2002 Colloidal inks for directed assembly of 3D periodic structures *Langmuir* **18** 5429–37
Studart A R 2016 Additive manufacturing of biologically-inspired materials *Chem. Soc. Rev.* **45** 359–76